

Effect of metal nanoparticle doping concentration on surface morphology and field emission properties of nano-diamond films

Yao Wang(王垚), Sheng-Wang Yu(于盛旺), Yan-Peng Xue(薛彦鹏), Hong-Jun Hei(黑鸿君), Yan-Xia Wu(吴艳霞), and Yan-Yan Shen(申艳艳)

Citation: Chin. Phys. B, 2021, 30 (**6**): 068101. DOI: 10.1088/1674-1056/abda33
Journal homepage: http://cpb.iphy.ac.cn; http://iopscience.iop.org/cpb

What follows is a list of articles you may be interested in

Influences of grain size and microstructure on optical properties of microcrystalline diamond films

Jia-Le Wang(王家乐), Cheng-Ke Chen(陈成克), Xiao Li(李晓), Mei-Yan Jiang(蒋梅燕), Xiao-Jun Hu(胡晓君)
Chin. Phys. B, 2020, 29 (**1**): 018103. DOI: 10.1088/1674-1056/ab593d

Preparation of patterned boron nanowire films with different widths of unit-cell and their field emission properties

Yong-Xin Zhang(张永欣), Fei Liu(刘飞), Cheng-Min Shen(申承民), Jun Li(李军), Shao-Zhi Deng(邓少芝), Ning-Sheng Xu(许宁生), Hong-Jun Gao(高鸿钧)
Chin. Phys. B, 2016, 25 (**8**): 088102. DOI: 10.1088/1674-1056/25/8/088102

Preparation of few-layer graphene-capped boron nanowires and their field emission properties

Yong-Xin Zhang(张永欣), Fei Liu(刘飞), Cheng-Min Shen(申承民), Tian-Zhong Yang(杨天中), Jun Li(李军), Shao-Zhi Deng(邓少芝), Ning-Sheng Xu(许宁生), Hong-Jun Gao(高鸿钧)
Chin. Phys. B, 2016, 25 (**7**): 078101. DOI: 10.1088/1674-1056/25/7/078101

Fluctuations of electrical and mechanical properties of diamond induced by interstitial hydrogen

Zhuang Chun-Qiang, Liu Lei
Chin. Phys. B, 2015, 24 (**1**): 018101. DOI: 10.1088/1674-1056/24/1/018101

Enhancing visible-light photocatalytic activity of α-Bi_2O_3 via non-metal N and S doping

Shang Jun, Gao Yuan, Hao Wei-Chang, Jing Xi, Xin Hui-Ju, Wang Liang, Feng Hai-Feng, Wang Tian-Min
Chin. Phys. B, 2014, 23 (**3**): 038103. DOI: 10.1088/1674-1056/23/3/038103

Effect of metal nanoparticle doping concentration on surface morphology and field emission properties of nano-diamond films*

Yao Wang(王垚)[1], Sheng-Wang Yu(于盛旺)[1], Yan-Peng Xue(薛彦鹏)[2], Hong-Jun Hei(黑鸿君)[1], Yan-Xia Wu(吴艳霞)[1], and Yan-Yan Shen(申艳艳)[1,†]

[1] *Institute of New Carbon Materials, Taiyuan University of Technology, Taiyuan* 030024, *China*
[2] *National Center for Materials Service Safety, University of Science and Technology Beijing, Beijing* 100083, *China*

(Received 29 October 2020; revised manuscript received 18 December 2020; accepted manuscript online 11 January 2021)

Nano-diamond particles are co-deposited on Ti substrates with metal (Ti/Ni) nanoparticles (NPs) by the electrophoretic deposition (EPD) method combined with a furnace annealing at 800 °C under N_2 atmosphere. Modifications of structural and electron field emission (EFE) properties of the metal-doped films are investigated with different metal NPs concentrations. Our results show that the surface characteristics and EFE performances of the samples are first enhanced and then reduced with metal NPs concentration increasing. Both the Ti-doped and Ni-doped nano-diamond composite films exhibit optimal EFE and microstructural performances when the doping quantity is 5 mg. Remarkably enhanced EFE properties with a low turn-on field of 1.38 V/μm and a high current density of 1.32 mA/cm^2 at an applied field of 2.94 V/μm are achieved for Ni-doped nano-diamond films, and are superior to those for Ti-doped ones. The enhancement of the EFE properties for the Ti-doped films results from the formation of the TiC-network after annealing. However, the doping of electron-rich Ni NPs and formation of high conductive graphitic phase are considered to be the factor, which results in marvelous EFE properties for these Ni-doped nano-diamond films.

Keywords: diamond films, metal doping, electrophoretic deposition, field emission properties

PACS: 81.05.uj, 85.45.Fd, 81.07.Wx **DOI:** 10.1088/1674-1056/abda33

1. Introduction

Diamond films have attracted much interest in studying the excellent electron field emission properties of vacuum microelectronic devices and flat panel displays. Besides its outstanding physical properties like high hardness, chemical inertness, high corrosion resistance, thermal conductivity, *etc*., diamond film possesses negative electron affinity and low effective work function, which thus have been widely studied for the applications in electron field emitters.[1–3] However, due to the high resistivity of diamond, the replenishment and transport of electrons in bulk diamond are diminished, it is difficult to form depletion regions required for rectification and modulation.[4–6]

Accordingly, some efforts have been made to improve the emission properties of diamond films, with most work focusing on surface treatments,[7,8] micropatterned structures,[9,10] and film doping.[11,12] It was reported that incorporation of metallic elements can not only effectively lower the residual stress and modify the carbon films' mechanical property, but also simultaneously improve the capability of field emission display (FED) cathode materials to emit electrons. For these reasons, diamond reinforced metal doped materials and their potential applications in electron field emission systems are extensively studied. For example, metal Ti can be bonded with diamond grains under certain annealing conditions to form a TiC structure or a layered structure with conductive channels.[13,14] The Ni ions have a certain degree of solubility to diamond and catalyze the formation of sp^2 carbon.[15–17]

However, detonated nano-diamond powder converted by carbon at high temperatures and high pressures[18] has been demonstrated to exhibit several special properties.[19] Moreover, electrophoretic deposition (EPD) could offer a more economical and simple method to produce not only a homogenous mixture of diamond and bonding phase particles which should fabricate continuous metal embedded diamond components, but also a controllable thickness coating. Therefore, it is expected to fabricate EFE enhanced Ti-doped and Ni-doped nano-diamond films by the EPD method.

In this work, different quantities of Ti or Ni nano-powders are doped in the nano-diamond films by the EPD method combined with a furnace annealing at 800 °C under N_2 atmosphere. Detailed studies are carried out to reveal the surface morphologies of the metal (Ti/Ni)-doped nano-diamond films by using field emission scanning electron microscope (SEM). The crystalline quality of the nano-diamond films is further investigated using x-ray diffraction (XRD) measurements and Raman spectroscopy. The x-ray photoelectron spectroscopy (XPS) measurements are performed on a PHI1600-ESCA system, with an incident radiation source of

*Project supported by the Science and Technology Major Project of Shanxi Province, China (Grant No. 20181102013) and the Fund from the "1331 Project" Engineering Research Center of Shanxi Province, China (Grant No. PT201801).

†Corresponding author. E-mail: shenyanyan@tyut.edu.cn

© 2021 Chinese Physical Society and IOP Publishing Ltd

Mg Ka ($h\nu = 1253.6$ eV) to reveal the chemical charge state of carbon of the nano-diamond film. It is found that appropriate doping concentration of metal (Ti/Ni) nano-powder can greatly improve the continuity and compactness, as well as the field emission properties of the nano-diamond films. The possible mechanisms for enhancing the EFE behaviors of the nano-diamond films are discussed based on these observations.

2. Experiment

In this work, 10 mm×10 mm×0.5 mm titanium sheets were used as the substrates. They were polished and cleaned by acetone, ethanol solution and deionized water in sequence before electrophoretic deposition. 40 mL of iso-butanol, 1 mL of acetone, 1 mL of deionized water, 20 mg of iodine, and 20 mg of nano-diamond powder were mixed as an electrophoresis solution required for the experiment. Then added into the solution were 2.5, 5, and 7.5 mg of Ti or Ni metal powders, respectively. The average grain size of Ti nanoparticles was in a range between 50 nm and 100 nm (99.8%, purity), the average grain size of Ni nanoparticles ranges from 50 nm to 100 nm (99.9%, purity). Each mixture was ultrasonically dispersed for approximately 60 min to form a suspension. In this experiment, the storage of the sample and the preparation of the solution were carried out in a glove box to prevent Ti and Ni powders from being oxidized.

The cathode and the anode were placed in the electrophoresis liquid, with their spacing being 10 mm. The treated Ti plate was fixed to the cathode by using a conductive paste and then the electrodes were put into the dispersed electrophoresis solution at a voltage of 60 V for 5 min. Then, Ti-doped and Ni-doped samples were annealed at 800 °C for 10 min in N_2 atmosphere to form Ti–C bonds between the diamond and the substrate to enhance bonding. The nano-diamond films doped with different quantities of Ti powders of 2.5, 5, and 7.5 mg were denoted as Ti2.5-D, Ti5-D, and Ti7.5-D, respectively. Similarly, the nano-diamond films doped with different quantities of Ni powders were named Ni2.5-D, Ni5-D, and Ni7.5-D, respectively. The undoped nano-diamond film without being annealed and undoped nano-diamond film with being annealed were also given for reference in this paper. They were called “pristine” and “as-prepared,” respectively.

Field emission scanning electron microscope (FE-SEM) was operated by combining with JSM-7100F/QX200 field emission scanning electron microscope. In the Raman spectroscopy, an argon laser beam was used to recognize the ‘structural’ quality of the nano-diamond film. The x-ray diffraction (XRD) data were measured with a scanning speed of 3 °/min and Cu $K\alpha$ radiation ($\lambda = 0.154$ nm). The EFE measurement was performed by a high vacuum field emission system built by Taiyuan University of Technology, where a slice of oxygen-free copper plate served as an anode, and the samples acted as a cathode, whereas the distance between the anode probe and the cathode nano-diamond films was 200 μm. When the vacuum reached 1.0×10^{-4} Pa, the current density *versus* electrical field (J–E) characteristic curve was measured by Keithley2290.

3. Results and discussion

Figures 1(a) and 1(b) show that the pristine films have poor uniformity with islands distributed on the surfaces of the nano-diamond films without metal doping. Clearly, after annealing in the N_2 atmosphere, an apparent continuous powder coating was deposited on the Ti surface. During annealing, due to solid-state diffusion-reaction,[20] the bonding reaction between the diamond and the Ti substrate occurred and produced a TiC transition layer.[13,14] Hence the bonding force between the Ti substrate and the diamond coating was enhanced, thereby improving the uniformity of the film. However, due to the unique surface properties and magnetism of diamond particles, particle agglomeration and deposition were easy to occur during electrodeposition, which not only weakened the uniform distribution of diamond particles in the coating, but also resulted in the appearing of the dome-shaped nodules, irregular gullies and grain coarsening, *etc*., in the coating. As a result, the microstructure of the coating was destroyed.[21]

Figures 2(a)–2(c) show the microstructures of the nano-diamond films doped with different quantities of Ti nano-powders. The surface morphologies of the films are remarkably changed by the doping of Ti powders. The islands completely disappear, the compactness and uniformity of the Ti-doped diamond films are significantly improved with the increasing of Ti concentration. However, many globular-shaped nodules (powder agglomerates) are visible on the diamond surface in the sample Ti2.5-D, which means that the agglomeration of diamond particles still happen at low concentration Ti doping. Studies show that the typical structure of a nano-diamond particle consists of a diamond core with a thin graphite shell, which stabilizes the particle.[21] As the content of Ti powders increases, diamond particles can be fully mixed with Ti particles, more and more Ti particles react with the graphite shell to form TiC between Ti particles and diamond grains (TiC interface). As a result, the bonding force between diamond grains, as well as between Ti substrate and diamond films is enhanced, which makes the surface of the sample continuous and dense. However, when the Ti doping amount reaches 7.5 mg, the sheet structures appear on the surface of the film, indicating the formation of TiC/Ti as shown in the EDS. They cover the effective emitters (diamond grains) and will diminish the field emission properties of the composited nano-diamond film.

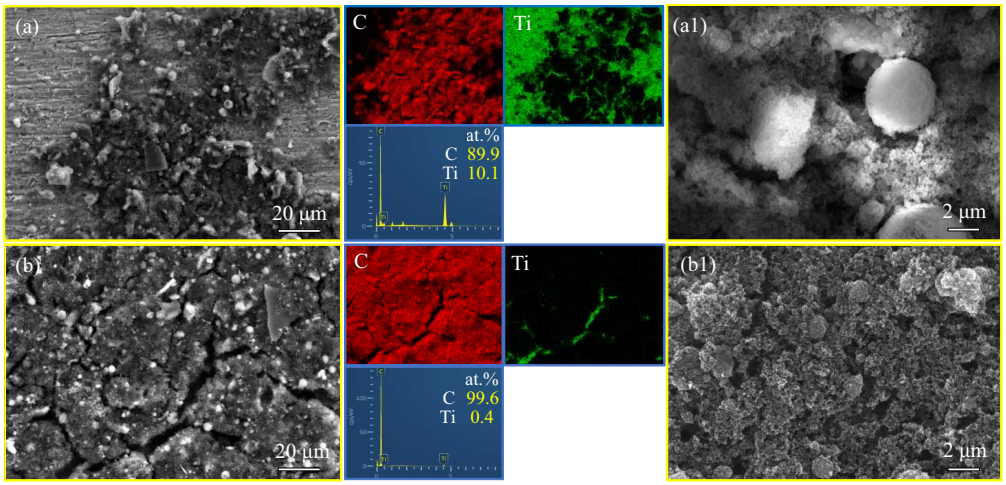


Fig. 1. FESEM images at 1 k× (left), EDS spectrum analysis (middle), and FESEM images at 10 k× (right) of (a) pristine and (b) as-prepared.

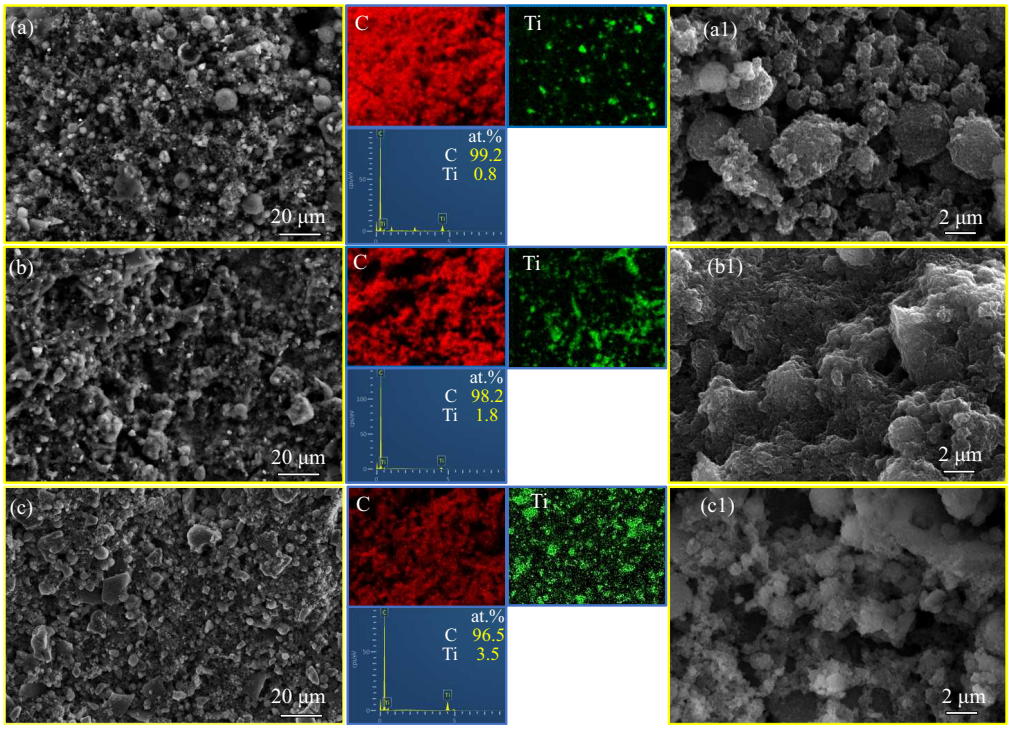


Fig. 2. FESEM images at 1 k× (left), EDS spectrum analysis (middle), and FESEM images at 10 k× (right) of (a) Ti2.5-D, (b) Ti5-D, and (c) Ti7.5-D.

Figures 3(a)–3(c) show SEM micrographs and EDS spectrum analysis for samples of Ni2.5-D, Ni5-D, and Ni7.5-D, respectively. The characteristics of the Ni-doped nano-diamond vary with the Ni doping concentration markedly, and the particle sizes of nano-diamond films can be tailored by controlling the amount of Ni in the electrolyte. A large number of Ni particles denoted as white dots are observed to be distributed in the Ni-doped nano-diamond films. It can be clearly seen through the EDS display at high magnifications (The figure is not shown here) that the large white particles in the picture are Ni particles. It can be found that the diameters of these Ni nanoparticles are about 50 nm–100 nm, which is similar to that of the Ni particle (80 nm in diameter) used in this study. Obviously, there still exist powder agglomerates and irregular gullies on the surface of the Ni2.5-D sample while the particles of the Ni5-D sample are uniform in size and compact in structure. It can be seen clearly from the high magnification SEM image that the Ni core is shielded by surrounding carbon elements (graphitic layers or amorphous carbon). However, when the Ni-doped content increases to 7.5 mg (Fig. 3(c)), the film is cracked into many sections. Even worse, the film shedding can be observed in some regions. Such a phenomenon is presumably ascribed to the worse diamond-to-substrate contact properties for the diamond film doped with excessive Ni powders. Meanwhile, the EDS patterns in Fig. 3 indicate that agglomerations of the Ni particles occur in the 7.5-mg Ni doping process, which will reduce the catalytic effect of Ni on diamond. Therefore, the field emission performance of diamond film can be expected to be reduced.

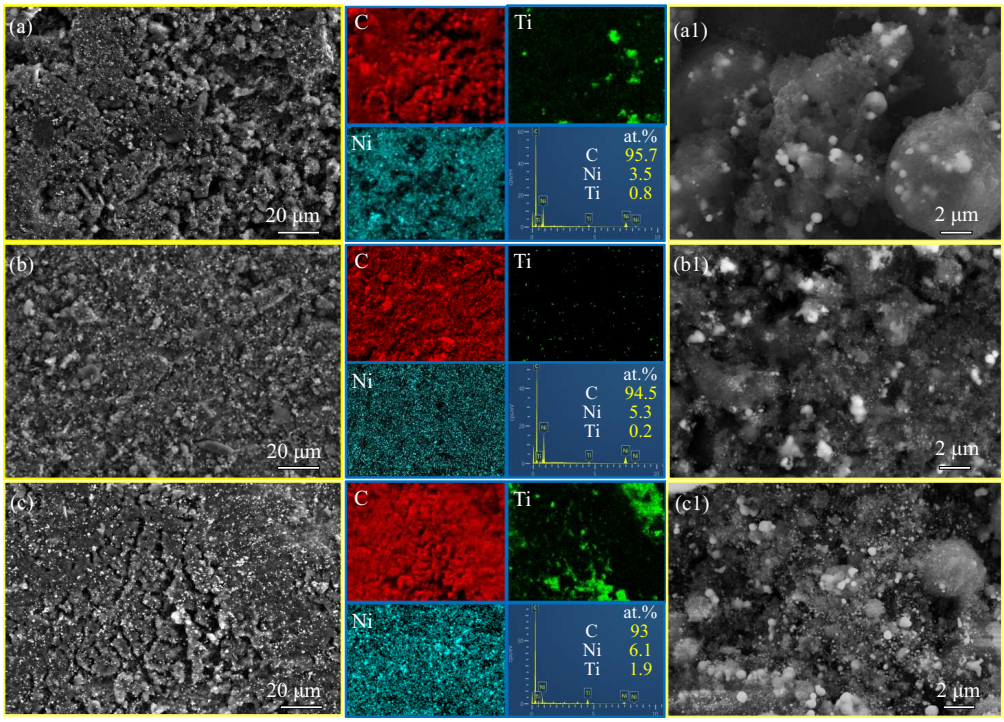


Fig. 3. FESEM images at 1 k× (left), EDS spectrum analysis (middle), and FESEM images at 10 k× (right) of (a) Ni2.5-D, (b) Ni5-D, and (c) Ni7.5-D.

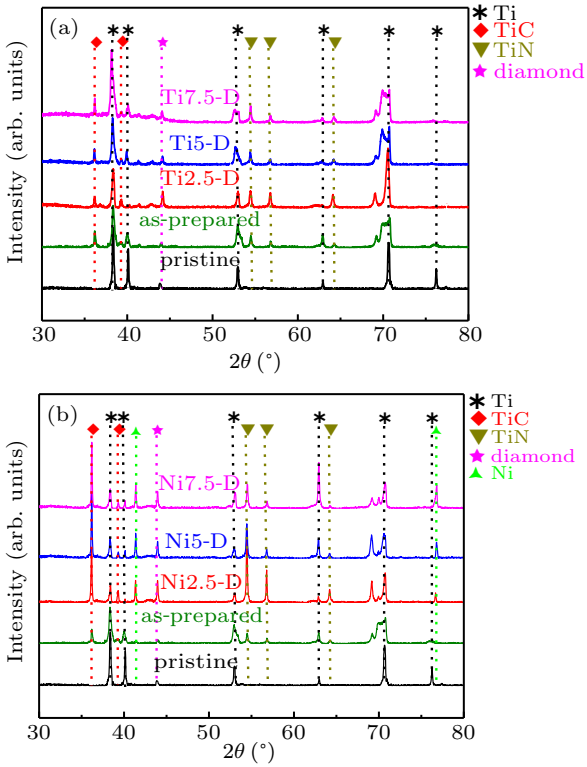


Fig. 4. (a) XRD patterns of pristine, as-prepared, Ti2.5-D, Ti5-D, and Ti7.5-D films; (b) XRD patterns of pristine, as-prepared, Ni2.5-D, Ni5-D, and Ni7.5-D films.

Figures 4(a) and 4(b) show the XRD patterns of the nano-diamond films doped with different quantities of Ti or Ni nano-powers. The peaks at $2\theta = 38.48°$, $40.17°$, $53.11°$, $62.95°$, $70.66°$, and $76.22°$ are attributed to reflections from Ti (002), (101), (102), (110), (300), and (112) lattice planes, respectively. The peak at $2\theta = 43.92°$ is assigned to the (111) lattice plane of the diamond, which indicates that the diamond films are successfully deposited on the Ti substrate by electrophoretic deposition.[22,23] Diffraction peaks at $2\theta = 36.1°$ and $39.37°$ appearing in all the annealed films demonstrate the existence of TiC, which indicates that the bonding reaction occurs between nano-diamond particles and Ti substrate in the annealing process and a good bonding (TiC layer) is realized.[24,25] Obviously, for the Ti-doped films, the intensities of the TiC peaks increase with the increasing of the content of Ti nano-powders, indicating that a larger number of TiC phases are generated between Ti NPs and diamond grains. In addition, the sample has diffraction peaks representing TiN compounds at $2\theta = 54.54°$, $56.74°$, and $64.27°$. This is because in the N_2 atmosphere at 800 °C, Ti-metal will react with N_2 to form TiN. As for these Ni-doped films, the peaks at $2\theta = 41.53°$, $76.7°$ are corresponding to Ni (002), (220),[26] which demonstrates that the Ni nanoparticles are successfully doped into nano-diamond films by electrophoretic deposition. As the Ni content increases, the intensity of the Ni diffraction peak increases continuously.

Figures 5(a) and 5(b) show the Raman spectra of the nano-diamond films doped with different quantities of Ti or Ni powders. The peak positions for samples are given in Table 1. Owing to their poor crystallinity and discontinuity, the signals related to pristine diamond peaks are very weak, so the original curve is magnified as given an insert. Raman spectra indicate that these films contain two main features: one is a broadened asymmetric peak which is superposed by 1325-cm^{-1} peak and 1350-cm^{-1} peak, with a shoulder shifting to-

ward lower wavenumbers, and the other is a broad peak with a maximum at about 1580 cm^{-1}. These diffused resonance peaks are typical characteristics observed for nano-diamond grains.[27,28] The D peak at 1325-cm^{-1} peak is assigned to diamond sp^3 bonded carbon while the D*-peak and G-peak, respectively, represent the disordered carbon and graphitic phase[10,14] contained in the diamond grains. Clearly, the diamond peak (1325 cm^{-1}) of the pristine nano-diamond film is shifted toward a lower frequency by 7 cm^{-1}, compared with the monocrystalline cubic diamond peak at 1332 cm^{-1}.[12] The phenomenon can be explained by a phonon confinement effect[29] and tensile stress of diamond.[30] Moreover, these tensile stress of diamond is also surmised to be an intrinsic stress.[31] After annealing, the D peak of the as-prepared film shows a shift from 3 cm^{-1} to a higher wavenumber of 1328 cm^{-1}, which means that the intrinsic stress of the diamond film decreases.[30]

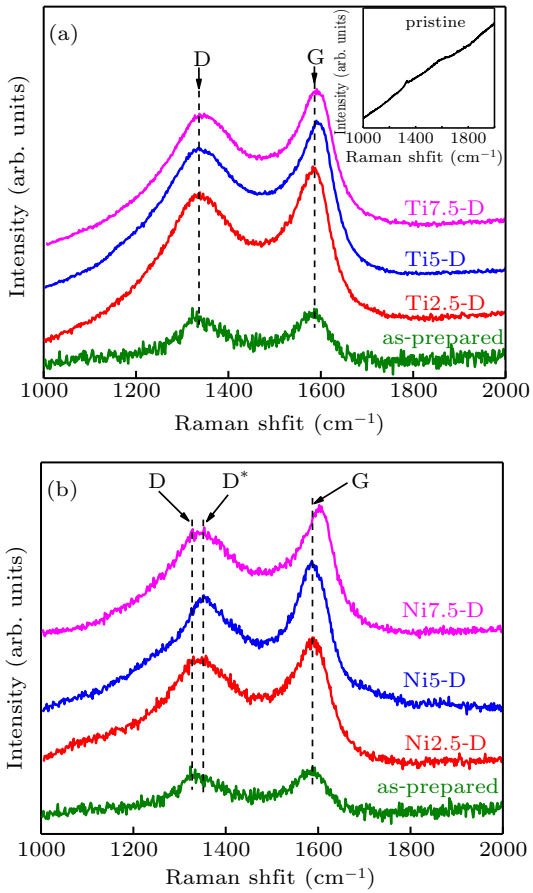


Fig. 5. (a) Raman spectra of as-prepared, Ti2.5-D, Ti5-D, Ti7.5-D films, with inset showing Raman spectrum of pristine; (b) Raman spectra of as-prepared, Ni2.5-D, Ni5-D, and Ni7.5-D films.

With the increasing of doping quantity of Ti nanoparticles, the D peak shifts unceasingly to a higher wavenumber and the peak value of D peak reaches 1332 cm^{-1}, which is consistent with the peak of the bulk diamond. Such a phenomenon is mainly because the ion doping will cause the stress of the nano-diamond film to decrease.[32] However, the D* peak shows a detectable increase in the Ni2.5-D film, which mainly because Ni has a certain solubility and catalytic capability for carbon materials, which is beneficial to converting part of the diamond into graphite phase.[15] Interestingly, the Raman signal of the diamond cannot be observed in the Ni5-D film due to the increase of graphitic or amorphous carbon catalyzed by Ni particles under 800 °C annealing, which will be further discussed in combination with XPS results. It should be noted that the visible Raman spectrum is over ten times sensitive to sp^2-bonds than to sp^3-bonds.[33] The fact that sp^2-signal is overwhelmingly larger than sp^3-signal in Raman spectrum does not mean that all of the sp^3-bonded materials have been converted into sp^2-bonded materials. However, when the doping quantity is further increased to 7.5 mg, the intensity of the D peak increases slightly. This can be explained by the agglomeration of Ni nanoparticles when the excessive Ni doping is applied as shown in Fig. 3(c), which reduces the catalytic effect of Ni on the diamond, resulting in a decrease in the number of disordered carbon or graphite phases.

Table 1. Peak positions for samples measured by Raman spectroscopy.

Sample	D peak (cm^{-1})	D* peak (cm^{-1})	G peak (cm^{-1})
Pristine	1325	1350	1580
As-prepared	1328	1353	1581
Ti2.5-D	1332	–	1585
Ti5-D	1333	–	1590
Ti7.5-D	1335	–	1592
Ni2.5-D	1331	1351	1590
Ni5-D	–	1352	1591
Ni7.5-D	1332	1353	1598

The XPS studies are carried out to investigate the modification of the chemical states and the near-surface characteristics of the nano-diamond films caused by doping different quantities of Ti or Ni powders. The C 1s photoemission spectra of the pristine, as-prepared, Ti or Ni-doped films are shown in Fig. 6. The measurement is conducted without ion sputtering etching to avoid reconfiguration of the bonds. The C 1s XPS peaks are deconvoluted by using a Lorentzian curve and the background contribution is removed by the Shirley's method.[34] Tracking the XPS core C 1s spectrum binding energy position, corresponding sp^2 (284.5 eV) and sp^3 (285.5 eV) intensities help to confirm our understanding of metal (Ti or Ni) doping-induced chemical and electrical behaviors. The data are fitted with Lorentzian peaks with binding energy at 284.4 eV and 285.1 eV corresponding to sp^2 and sp^3 bonds,[35] and their relative intensities are given in Table 2. In the pristine film, sp^3 bonding is predominant with a peak intensity of 57.34%, while sp^2 intensity is 42.66%. After annealing process in N_2 atmosphere, the slight decline in the sp^2 intensity means that the graphite shell reacts with the Ti substrate to form TiC.[36] Additionally, sp^2 peak intensity exhibits continuous decrease with the increase of Ti doping content, which

further verifies that the sp^2 carbon rather than sp^3 carbon is consumed to generate TiC. However, for the Ni-doped film, the peak intensity of sp^2 of the Ni5-D increases to 67.53%, which further confirms that the Ni particles catalyze a certain amount of sp^3 to sp^2. Interestingly, compared with Ni5-D, excessive doping of Ni powders (7.5 mg) results in the intensity of the sp^2 peak decreasing slightly. The XPS results are well consistent with the Raman results.

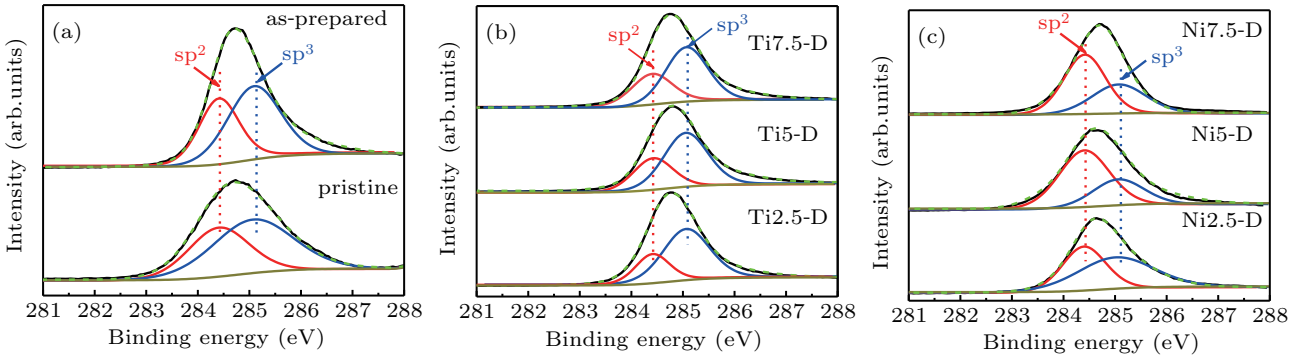


Fig. 6. (a) C 1s XPS spectra of pristine and as-prepared; (b) C 1s XPS spectra of Ti2.5-D, Ti5-D, and Ti7.5-D; (c) C 1s XPS spectra of Ni2.5-D, Ni5-D, and Ni7.5-D.

Table 2. Relative intensities of various components of C 1s XPS spectra for pristine, as-prepared, Ti2.5-D, Ti5-D, Ti7.5-D, Ni2.5-D, Ni5-D, and Ni7.5-D samples.

Peak position (eV)	Chemical bonding	Peak intensity (%)							
		Pristine	As-prepared	Ti2.5-D	Ti5-D	Ti7.5-D	Ni2.5-D	Ni5-D	Ni7.5-D
284.4	sp^2	42.66	40.69	34.04	30.22	28.89	60.08	67.53	65.13
285.1	sp^3	57.34	59.31	65.96	69.78	71.11	39.32	32.47	34.87

Figure 7 shows the *J*–*E* curves and the FN plots of the EFE characteristics obtained from the diamond films doped with different quantities of Ti and Ni nano-powders. The details of the field emission parameters, such as turn-on field (E_0) and EFE current density (J_e) are given in Table 3. The turn-on field (E_0) is designated as the interception between the high- and low-field line segment of the FN plots.[27] Owing to the discontinuity and higher resistivity of the diamond grains, the pristine film exhibits diminished emission properties. The field emission performance shows that 800 °C annealing effectively lowers the turn-on field from 8.15 V/μm to 6.46 V/μm and increases the emission current density to 13.46 μA/cm^2 under 7.12 V/μm. Obviously, there is a significant variation in the emission characteristics for diamond doped with different quantities of metal (Ti/Ni) powders compared with those for the un-doped diamond films. With the increase of the doping metal quantity, the EFE properties of the metal doped-diamond films first increase and then decrease. For the Ti-doped nano-diamond films, remarkably enhancement in EFE properties is observed in Ti5-D film, which shows a low turn-on field of 3.04 V/μm and a current density of 15.54 μA/cm^2 at an applied field of 3.69 V/μm. Interestingly, the Ni5-D film possesses an optimal EFE property with nickel incorporation. Its turn-on field is reduced to 1.38 V/μm, and a high current density of 1.32 mA/cm^2 at an applied field of 2.94 V/μm is obtained, which are superior to those of Ti-doped film. But the excessive doping of metal powders (7.5 mg) reduces the EFE properties of the nano-diamond film.

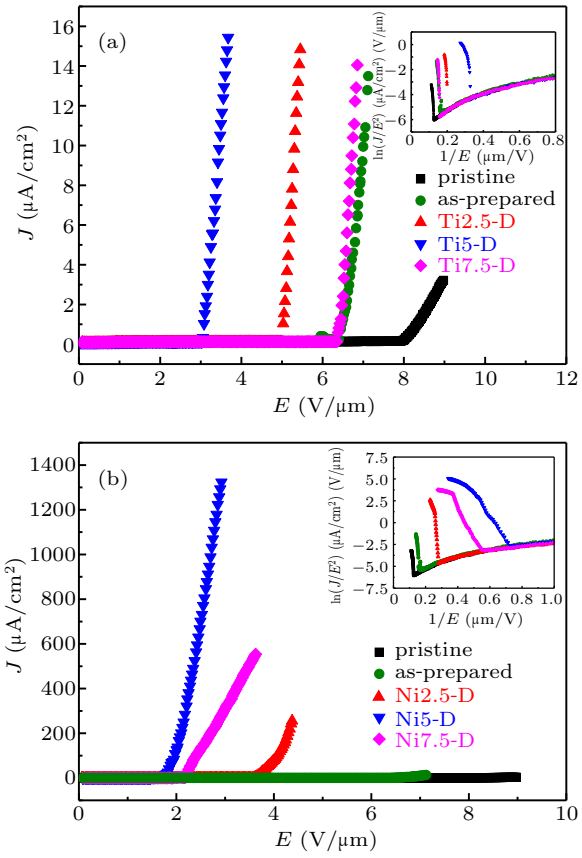


Fig. 7. (a) Electron field emission properties of pristine, as-prepared, Ti2.5-D, Ti5-D, and Ti7.5-D films; (b) electron field emission properties of pristine, as-prepared, Ni2.5-D, Ni5-D, and Ni7.5-D films, where insets show corresponding Fowler–Nordheim (FN) plots.

Table 3. Data on turn-on field (E_0), EFE current density (J_e), and applied field (E) for nano-diamond films corresponding to samples of Fig. 7.

Sample	E_0 (V/μm)	J_e (μA/cm^2)	E (V/μm)
Pristine	8.15	3.22	9.12
as-prepared	6.46	13.46	7.12
Ti2.5-D	4.94	13.26	5.44
Ti5-D	3.04	15.54	3.69
Ti7.5-D	6.29	14.16	6.86
Ni2.5-D	3.61	268.98	4.38
Ni5-D	1.38	1323.47	2.94
Ni7.5-D	4.54	201.55	6.59

Based on the above results from SEM, XRD, and Raman measurements, the conduction mechanism for the improved conductivity can be discussed below.

The discontinuity of the nano-diamond film makes it impossible for the electrons to be continuously released in the transmission process, thus the pristine film shows poor field emission properties. After 800-°C annealing, the formation of TiC transition layers between the diamond films and the Ti plate improves the uniformity of the sample, which increases the number of emission sites (diamond grains) on the surface of the film. Meanwhile, the formation of TiC generates the ohmic contact between Ti and diamond, lowering the interface barrier effectively, which makes it easier for electrons to be transported from the Ti plate to the diamond. In the case of Ti-doped nano-diamond film, diamond particles can be fully mixed with Ti particles, hence more and more TiC interfaces are formed between Ti particles and diamond grains. As a result, a TiC-network will be built between diamond grains, as well as between Ti substrate and diamond films.[36] The formation of the TiC-network allows the electrons to be easily transferred from the TiC to the diamond surface layer and then emitted into vacuum from the diamond surface. However, the excessive doping of Ti powders makes the surface of the film covered with a large amount of Ti or/and TiC, reducing the number of effective emitters and thus diminishing the field emission properties.

For the Ni-doped films, on the one hand, Ni particles can effectively promote the conversion of diamond phase (sp^3 carbon) into high conductive graphite phase (sp^2 carbon), which is beneficial to the EFE properties. On the other hand, researchers found that these metallic NPs are rich in electrons, which can act as "conductive islands" and benefit the electron transportation.[37,38] Consequently, the electrons are transported easily through the graphitic phases and Ni NPs as well as through the conduction channels of the diamond grains to the emitting surface, then emitted to vacuum without any difficulty as the diamond surface is negative electron affinity in nature. Hence, we deduce that the incorporation of Ni NPs and the increase of graphitic phases are the factors for the enhanced EFE properties of the Ni-doped nano-diamond films.

4. Conclusions

Nano-diamond powders doped with metal (Ti/Ni) powders are coated onto Ti substrates by an electrophoretic deposition method, followed by an annealing treatment at 800 °C. Microstructural and EFE properties of the obtained metal-doped diamond composite coating first increase and then decrease as the doping concentration of the metal (Ti/Ni) powders increases. Both the Ti-doped and Ni-doped nano-diamond films yield excellent surfaces and EFE properties at an appropriate doping quantity of 5 mg. On the one hand, the enhancement of the EFE properties of the Ti-doped films originates from the formation of TiC-network after being annealed. However, excessive Ti nanoparticle doping will generate a large amount of TiC/Ti covering the surface of the diamond film, which reduces the effective emission particles of the diamond surface and leads the field emission properties to degrade. On the other hand, electron-rich Ni nanoparticle acts as a "conductive island" and effectively promotes the conversion of nano-diamond into high conductive graphite phase, which results in excellent EFE properties for these Ni-doped nano-diamond films. Otherwise, excessive doping of Ni powders induces the Ni particles to agglomerate, which weakens the catalytic effect and damages the continuity of the diamond film. As a result, the field emission properties are reduced.

References

[1] Zhu W, Kochanski G P and Jin S 1997 *MRS Proc.* **509** 53
[2] Okano K, Hoshina K, Iida M, Koizumi S and Inuzuka T 1994 *Appl. Phys. Lett.* **64** 2742
[3] Yang W L, Fabbri J D, Willey T M, Lee J R, Dahl J E, Carlson R M, Schreiner P R, Fokin A A, Tkachenko B A, Fokina N A, Meevasana W, Mannella N, Tanaka K, Zhou X J, van Buuren T, Kelly M A, Hussain Z, Melosh N A and Shen Z X 2007 *Science* **316** 1460
[4] Yu H Y, Gao N, Li H D, Huang X R, Duan D F, Bao K, Zhu M F, Liu B B and Cui T 2019 *Chin. Phys. B* **28** 088102
[5] Geis M W, Twichell J C, Macaulay J and Okano K 1995 *Appl. Phys. Lett.* **67** 1328
[6] Tse K Y, Nichols B M, Yang W, Butler J E, Russell-J J N and Hamers R J 2005 *J. Phys. Chem. B* **109** 8523
[7] Lee Y C, Pradhan D, Lin S J, Chia C T, Cheng H F and Lin I N 2005 *Diamond Relat. Mater.* **14** 2055
[8] Dong C L, Chen S S, Chiou J W, Chen Y Y, Guo J H, Cheng H F, Li I N and Chang C L 2008 *Diamond Relat. Mater.* **17** 1150
[9] Subramanian K, Kang W P, Davidson J L, Jarvis J D, Hofmeister W H, Choi B K and Howell M 2006 *Diamond Relat. Mater.* **15** 417
[10] Raina S, Kang W P and Davidson J L 2008 *Diamond Relat. Mater.* **17** 790
[11] Hu X J, Hu H, Chen X H and Xu B 2011 *Acta Phys. Sin.* **60** 068101 (in Chinese)
[12] Xu Hui, Liu J J, Ye H T, Coathup D J, Khomich A V and Hu X J 2018 *Chin. Phys. B* **27** 096104
[13] Yang Y N, Zhang Z Y, Zhang F C, Dong J T, Zhao W, Zhai C X and Zhang W H 2012 *Chin. Phys. Lett.* **29** 18103
[14] Zhai C X, Yun J N, Zhao L L, Zhang Z Y, Wang X W and Chen Y Y 2011 *Physica B* **406** 1124
[15] Lee E C and Choi J W 2001 *Surf. Coat. Technol.* **148** 234
[16] Carey J D, Forrest R D, Khan R U A and Silva S R P 2000 *Appl. Phys. Lett.* **77** 2006
[17] Smirnov W, Hees J J, Brink D, Muller-Sebert W, Kriele A, Williams O A and Nebel C E 2010 *Appl. Phys. Lett.* **97** 073117

[18] Chen Q and Yun S 2000 *Mater. Res. Bull.* **35** 1915
[19] Gneiner N R, Phillips D S, Johnson J D and Volk F 1988 *Nature* **333** 440
[20] Wada N and Solin S A 1981 *Physica B* **105** 353
[21] Barnard A S and Sternberg M 2007 *J. Mater. Chem.* **17** 4811
[22] Chaure S, Chaure N B, Hassan A K, Ray A K, Reehal H S, Ghermazion A and Capan R 2005 *Vacuum* **77** 231
[23] Ali M and Ürgen M 2011 *Appl. Surf. Sci.* **257** 8420
[24] Zhang C Z, Li Y S, Tang Y, Yang L, Zhang L, Sun Y, Yang Q and Hirose A 2013 *Thin Solid Films* **527** 59
[25] Tachibana T, Williams B E and Glass J T 1992 *Phys. Rev. B* **45** 11975
[26] Kumar S and Chakarvarti S K 2004 *J. Mater. Sci.* **39** 3249
[27] Wang R Z, Wang B and Yan H 2002 *Physics* **31** 84 (in Chinese)
[28] Vadym M, Sebastian O and Yury G 2009 *Chem. Mater.* **21** 273
[29] Yoshikawa M, Mori Y, Obata H, Maegawa M, Katagiri G, Ishida H and Ishitani A 1995 *Appl. Phys. Lett.* **67** 694
[30] Pu M F, Zhang F, Liu S, Irifune T and Lei L 2019 *Chin. Phys. B* **28** 053102
[31] Nijhawan S, Jankovsky S M and Sheldon B W 1995 *MRS Proc.* **416** 163
[32] Chen S L, Shen B, Zhang J G, Wang L and Sun F H 2012 *Trans. Nonferrous Met. Soc. China* **22** 3021
[33] Chen H C, Teng K Y, Tang C Y, Balakrishnan S, Sankarakumar A and Lin I N 2010 *J. Appl. Phys.* **108** 123712
[34] Panda K, Sundaravel B, Panigrahi B K, Magudapathy P, Nandagopala K D, Nair K G M, Chen H C and Lin I N 2011 *J. Appl. Phys.* **110** 44304
[35] Chen Y F 1996 *Surf. Sci.* **380** 199
[36] Zhai C X, Zhang Z Y, Zhao L L, Wang X W and Zhao W 2015 *Thin Solid Films* **574** 10
[37] Wu Y G, Zhang T H, Liu A D and Zhou G 2002 *Surf. Coat. Technol.* **157** 262
[38] Shen Y Y, Qi T, Qiao Y, Hei H J, He Z Y and Yu S W 2016 *Vacuum* **123** 160